

1 Type of the Paper: Proceedings

2 Impact of the assimilation of non-precipitating echoes 3 reflectivity data on the short-term numerical forecast of SisPI. †

4 Adrian Luis Ferrer Hernández ^{1,*}, Pedro Manuel González Jardines ¹, Maibys Sierra Lorenzo ¹ and Darielis de la
5 Caridad Aguiar Figueroa ¹

6 ¹ Center for Atmospheric Physics, Institute of Meteorology, Havana, Cuba

7 * Correspondence: Ferrer, A.L. aluislfh@gmail.com

8 † Presented at the 5th International Electronic Conference on Atmospheric Sciences, 16-31 July 2022.

9 **Abstract:** The research carries out an evaluation of the 3DVAR method with different options for
10 the assimilation of reflectivity data, which are applied to the SisPI system with the purpose of
11 determining which scheme presents the best results in the short-term numerical weather
12 prediction. For this, data from 6 meteorological radars with coverage over a domain with 3km of
13 spatial resolution are used, using the indirect method with (3DVAR-NoRain) and without
14 (3DVAR) activate an option to also consider null-echoes of reflectivity without presence of
15 precipitation. As a test case, the cold front that affected Cuba on December 10th, 2018 is taken.

16 **Keywords:** Data Assimilation; Numerical Weather Prediction; Mesoscale.

17

Citation: Ferrer, A.L.; González, P.M.; Sierra, M.; Aguiar, D. Impact of the assimilation of non-precipitating echoes reflectivity data on the short-term numerical forecast of SisPI. *Environ. Sci. Proc.* **2022**, *4*, 21. <https://doi.org/10.3390/ecas2022-061103>

Academic Editor: Anthony Lupo

Published: June, 2022

Publisher's Note: MDPI stays neutral with regard to jurisdictional claims in published maps and institutional affiliations.



Copyright: © 2022 by the authors. Submitted for possible open access publication under the terms and conditions of the Creative Commons Attribution (CC BY) license (<https://creativecommons.org/licenses/by/4.0/>).

1. Introduction

The short-term numerical weather prediction system (SisPI for its acronym in Spanish) [1,2,3] is one of the operational models that are implemented in the Institute of Meteorology of Cuba (INSMET). The SisPI uses the Weather Research & Forecast (WRF) [4] model as atmospheric core. The design of this system [1] takes into account the development of a module for data assimilation of different types of meteorological observations. For this reason, this work approaches the weather forecasts from the point of view of the data assimilation, explaining how the insertion of a new data source such as meteorological radars can improve the initial conditions and subsequently the result of the simulation.

The first steps in the assimilation of radar data in Cuba were through the work of Hernández (2013) and Ferrer (2013), where the ARPS model was initialized with data from the Key West (KBYX) radar and INSMET meteorological stations. Subsequently, in the work of Sierra et al. (2014), the WRFDA module is used for the first time with eolic gradient towers and surface stations in LittleR format in Cuba. Subsequently, Armas (2015) used the WRFDA with data from polar orbiting satellites and meteorological observations in PrepBufr format from the NOAA GDAS system. Ferrer and Borrajero (2019) implemented a converter from the Nexrad Level II radar data format to the FM-128 format required by the WRFDA module [4]. In this work, authors made experiments carried out with different types of covariance matrices with the options CV3, CV5 and CV7, obtaining the best results with this last option CV7.

Subsequently, Fernández (2019) carried out experiments for the assimilation of radar data with the 3DVAR method and different window sizes in the construction of the covariance matrices. Other recently highlighted work is González et al. (2021). In this work, authors evaluated for the first time in Cuba different methods such as 3DVAR, 3DEnVAR and 4DEnVAR, sticking out its advantages and the best results obtained with hybrid schemes, with which the advantages can be appreciated over 3DVAR method, because the contribution of the members of the ensemble provided information about hydrometeors control variables even in areas where radar data is not available.

Finally, there is the work of Aguiar (2021), in which he evaluates different options implemented in the WRFDA for the assimilation of reflectivity data, highlighting the indirect method with the inclusion of hydrometeors. These last works have been limited only to the use of NOAA radar data, hence in this work it was decided to make efforts to use complete coverage throughout the maximum resolution domain of SisPI, with also data from the radar network of the INSMET. On the other hand, the main objective of this research is to evaluate the impact of assimilating reflectivity data of non-precipitating echoes (radar_non_precip_opt parameter of WRFDA namelist [4]) in the short-term numerical weather forecast of SisPI. This is a recently available option in the WRFDA module implemented by Min & Kim (2016), and nowadays its use in the country has not been evaluated. In turn, it is also intended to carry out an experiment in which a total coverage of reflectivity information can be available in the domain of maximum spatial resolution. A null-echo is defined as a region with non-precipitation echoes within the radar observation range. The model removes excessive humidity and four types of hydrometeors (wet and dry snow, graupel, and rain) based on the radar reflectivity by using a three-dimensional variational (3D-Var) data assimilation technique within the WRFDA system [13].

2. Materials and Methods

For the accomplishment of this work the WRF-ARW model (version 4.1.2) and the WRFDA module (version 4.3) are used [4]. The physical configurations taken into account in the model were defined by Sierra et al. (2014 and 2017) and Alfonso et al. (2021). The WRFDA configuration was based on researches of Gonzalez et al. (2021) and Aguiar (2021). The assimilation of satellite and prepbufr data from the GDAS system is carried out for all domains (27, 9, and 3 km spatial resolution). In the case of domain 3 (3 km), data from the INSMET and NOAA radar network (KBYX and KAMX) are also assimilated, guaranteeing with this a total coverage of reflectivity information on the domain of maximum spatial resolution.

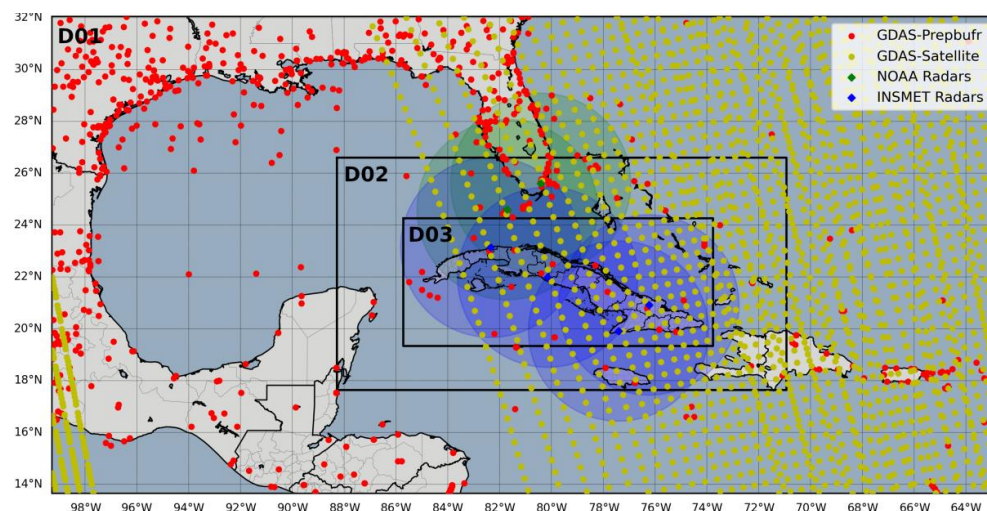


Figure 1. Domain configuration and meteorological observations used.

The WRF model was initialized from GFS (Global Forecast System) forecast data with 0.5° horizontal resolution. A radar data conversion tool in Nexrad Level II format to FM-128 format implemented in Python by Ferrer and Borrajero (2019) is employed. The 3D-Var data assimilation method used in WRF system [14] is capable of assimilating all types of conventional observations, as well as radar data. The 3D-Var system combines the observations with background information on the model state and uses a linearized forecast model to ensure that the observations are given a dynamically realistic and consistent analysis field [15]. The domain-dependent covariance matrix (BECs) used (CV7) was generated with the inclusion of hydrometeors and vertical velocity as control variables with a 1 month of period of WRF (SisPI) outputs (initializations cycles of 0000 and 12000 UTC). Multiple outer loops (max_ext_its = 3) are utilized, where the multiplicative weight of its control variables is also modified (var_scaling = 1.0-0.5-0.25, len_scaling = 1.0-0.5-0.25). Table 1 describes the number of assimilated observations in each domain of the WRF model for the selected test case.

Table 1. Number of assimilated observations in each simulation domain.

OBS Types	Domain 01	Domain D02	Domain D03
Airep	8	-	-
Soundings	15	4	-
Metar	325	32	11
Ship	43	21	9
Synop	76	10	3
Buoy	123	11	-
Radiance	1909	438	153
Radar	-	-	2404
Total	2499	516	2580

As a test case, the cold front that affected the western region of Cuba on December 10th, 2018 is taken, which was preceded by a prefrontal squall line that caused heavy rains on the north coast of Havana with significant accumulations in less than three hours. The satellite image (Figure 2a) shows a frontal system that extends from a low-pressure center located on the east coast of the United States to Yucatan and the Gulf of Campeque. This cold front is preceded by low clouds that move over the Gulf of Mexico and the vicinity of the western region of Cuba. Ahead of this cold front, a line of storms can be seen, shown in the radar image (Figure 2b), which put on display reflectivity echoes from storm areas over Havana.

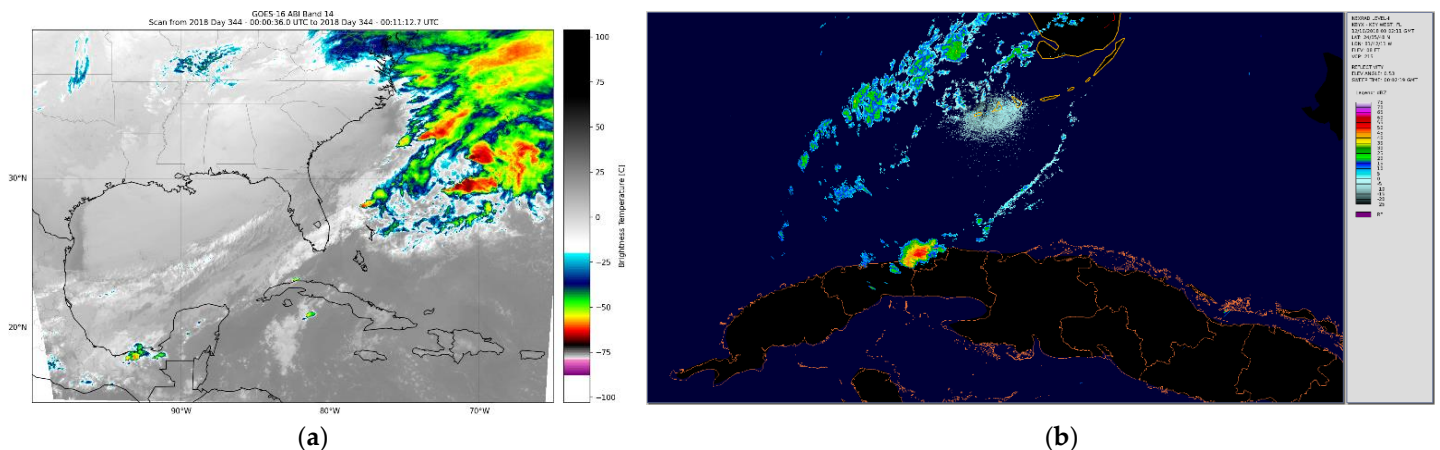


Figure 2. Test case of December 10th, 2018 at 0000 UTC: (a) GOES-16 (Channel 14) infrared image and (b) KBYX Radar reflectivity observation (Key West, Florida) at 0.5 elevation angle.

104

Table 2. Experimental design.

Experiment name	Description
NoDA	No data assimilation
3DVAR	GFS + GDAS + Radar
3DVAR_noRain	GFS + GDAS + Radar + Null echoes

105

106

107

108

109

110

111

112

113

114

115

116

117

118

Table 2 describes the experiments design to be carried out. Simulations without data assimilation (NoDA) are compared with simulations with (3DVAR noRain) and without (3DVAR) activate the radar_non_precip_opt option. For this, the calculation of metrics and obtaining maps from the simulated and observed meteorological variables is implemented in the Python programming language. For the evaluation of the experiments, 68 surface meteorological stations of the Institute of Meteorology, GOES-16 images, and Radar Observations were used. The radar data employed was acquired from <https://www.ncdc.noaa.gov/nexradinv/index.jsp>, GOES-16 data was used from https://home.chpc.utah.edu/~u0553130/Brian_Blaylock/cgi-bin/goes16_download.cgi, and while the rest of the Bufr observation data and the GFS global model outputs were downloaded from <https://rda.ucar.edu/>.

119

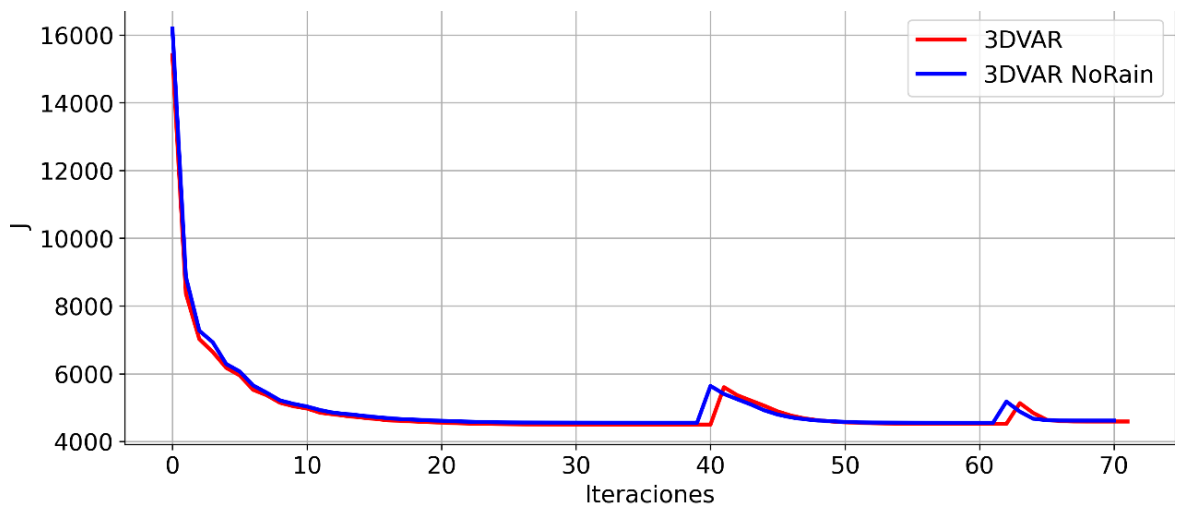
3. Results Discussion

120

121

Through the use of multiple outer loops, it is observed that the resulting cost functions show a great similarity, although the 3DVAR-NoRain configuration tends to minimize this function in fewer iterations (Figure 3).

122



123

Figure 3. Comparison of the cost functions of the experiments carried out.

124

125

126

127

128

129

130

131

132

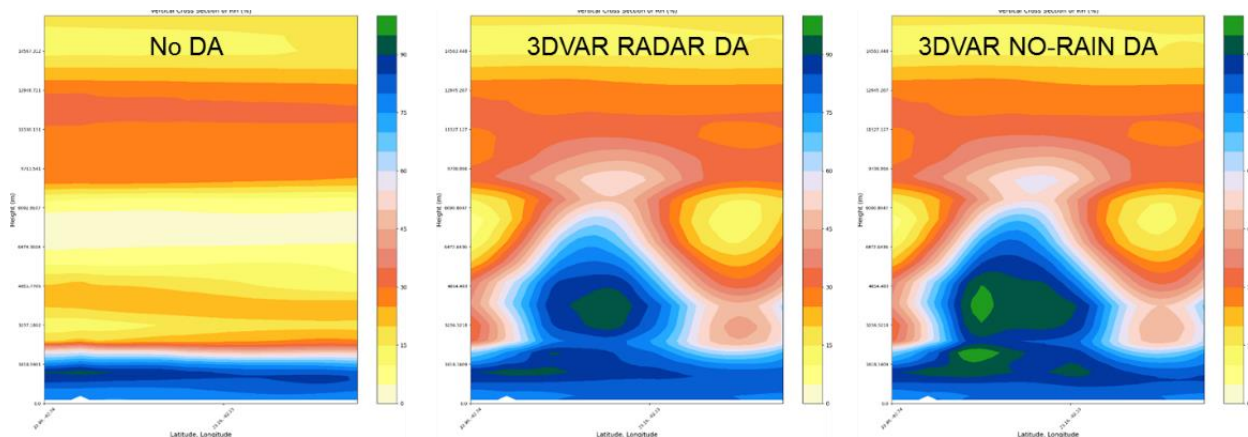
133

134

Making vertical cross-sections in the relative humidity initialization fields for the different experiments, it can be seen over Havana in the case of simulations without data assimilation (No DA), how these are not taken into account the influence on the vertical structure of the cloudy areas that are present in the study area. This is because they are the result of initializing only with low spatial resolution information from the GFS model, without inserting radar data or other observations types. On the other hand, both simulations with radar data assimilation insert the influence of cloudy areas in the vertical structure of the relative humidity analysis fields obtained, which can be seen in Figure 4. In the comparison of vertical cross-sections between the experiments with data assimilation, few differences are shown between them, although in the case of 3DVAR-noRain an increase in the spatial distribution of relative humidity inside the cloud is

135
136

observed, obtaining a more realistic structure of the convective storm present at the time of model initialization.



137
138
139

Figure 4. Vertical cross sections of the relative humidity of experiments with and without radar data assimilation.

140
141
142
143
144
145
146
147
148
149

The comparison of the behavior of the brightness temperature values measured by the GOES-16 satellite corresponding to the first periods of the simulations (Figure 5), shows that the 3DVAR-noRain experiment obtained a greater ability to predict the areas of convective cloudiness associated with the prefrontal squall line, which maintained activities of convective storm areas in the sea at the north of Havana hours after the moment of initialization of the model. On the other hand, the 3DVAR experiment (without the radar_non_precip_opt option) attenuated the development of the convective process and did not adequately reflect the evolution of the clouds pattern associated with the squall line, which may be linked to differences in relative humidity analyses fields described in Figure 4.

150
151
152
153
154

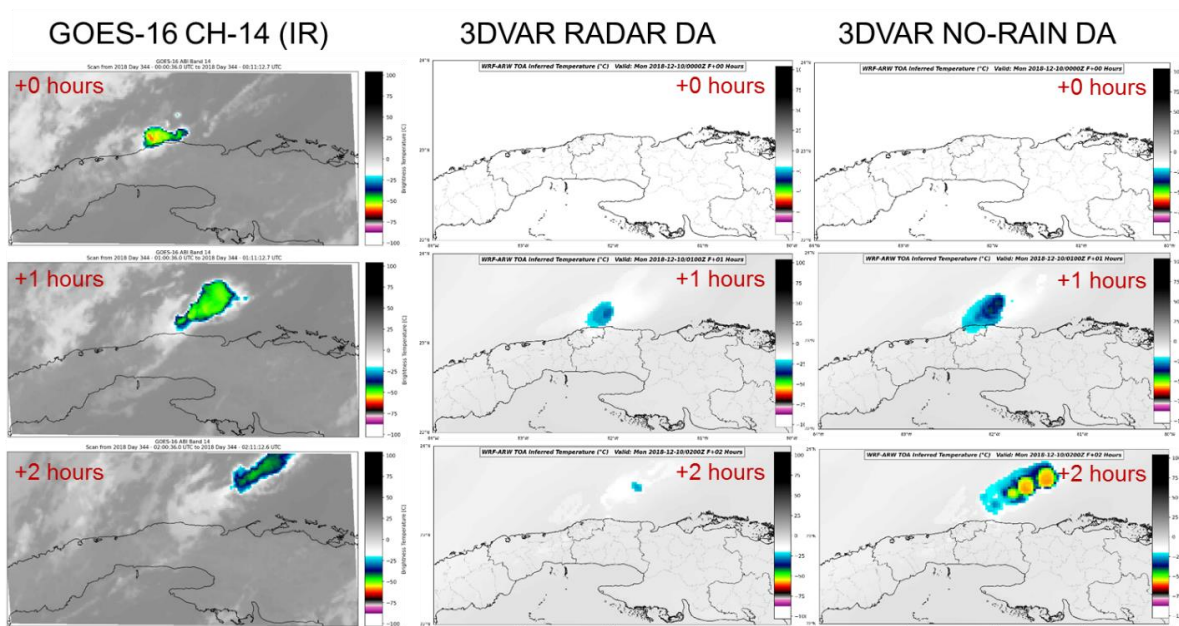
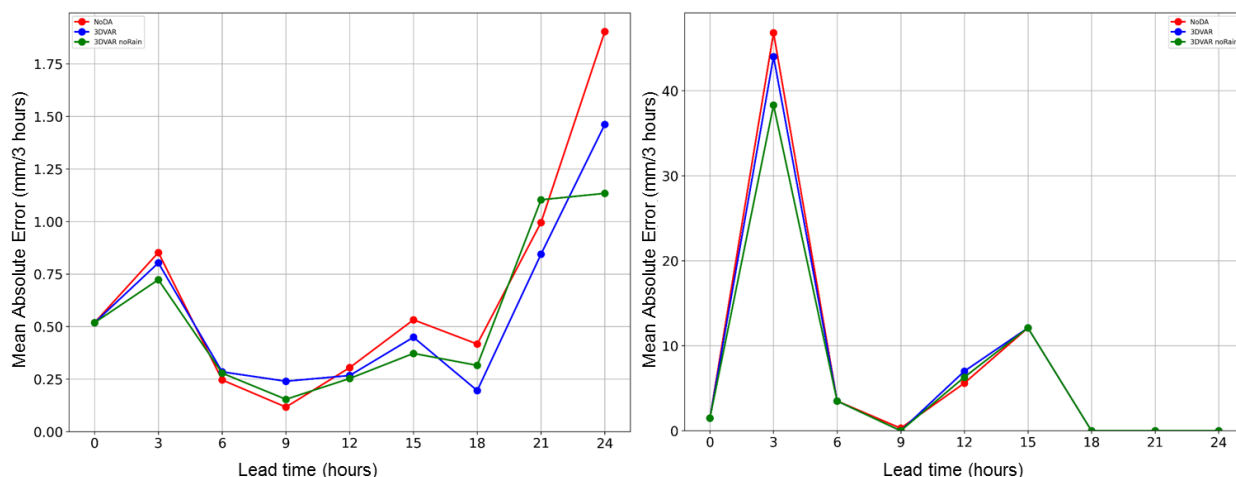


Figure 5. Comparison of the temperature of the cloud tops observed by the GOES-16 satellite with respect to the outputs of the WRF model assimilating radar data with (3DVAR noRain) and without (3DVAR) activating the null-echoes option during the first 2 hours of simulation.

155
156
157
158
159
160
161
162
163

In comparison with 3-hourly precipitation observations of the INSMET stations network (Figure 6a) and also specifically with the station of Casablanca (Havana) (Figure 6b), which was affected by the rainfall associated with the prefrontal squall line, it was possible to determine that despite of the similar behavior of all the simulations, differences are observed in the first hours of the run, seeing that the 3dvar-noRain experiment presented slightly lower mean absolute error values with respect to the rest of the simulations. These mean values during the simulation period ranged between 0.2 and 1.8 mm/3h (Figure 6a) and between 0 and 48 mm/3h (Figure 6b) for the case of accumulated precipitation measured at the Casablanca station.



164
165
166
167

Figure 6. Mean Absolute Error (mm/3 hours) of precipitation forecast: (a) Verification with 68 synoptic stations of INSMET and (b) Verification with Casablanca (La Habana) synoptic station (WMO 78325).

168
169

4. Conclusions

170
171
172
173
174
175
176
177
178
179

The Null-echoes assimilation option proved to be an important option in the assimilation of radar data. It allows more realistic construction of moisture fields and its vertical structure in areas of observed reflectivity echoes. The use of this option contributes to improving the precipitation forecast and adequately reproduces the convective processes in the first time steps. The simulation with radar data assimilation but without the use of this option did not adequately represent the reflectivity echoes and the brightness temperatures of cloud tops in the first 2 hours of simulation. The verification with synoptic stations data showed that the use of the radar_non_precip_opt option made it possible to obtain lower Mean Absolute Error values in the forecast of accumulated precipitation in the first 3 hours of simulation.

180
181
182
183
184
185

Author Contributions: Conceptualization, M.S.L. and P.M.G.J.; methodology, P.M.G.J.; software, A.L.F.H.; validation, A.L.F.H.; formal analysis, A.L.F.H., D.C.A.F., M.S.L. and P.M.G.J.; investigation, D.C.A.F. and A.L.F.H.; resources, M.S.L.; data curation, A.L.F.H.; writing—original draft preparation, A.L.F.H.; writing—review and editing, A.L.F.H.; visualization, A.L.F.H.; supervision, M.S.L. and P.M.G.J.; project administration, M.S.L.; funding acquisition, M.S.L.. All authors have read and agreed to the published version of the manuscript.

186

Conflicts of Interest: The authors declare no conflict of interest.

References

188
189
190

- Sierra-Lorenzo, M., Ferrer-Hernández, A. L., Hernández-Valdés, R., González-Mayor, Y., Cruz-Rodríguez, R. C., Borrajero-Montejo, I. and Rodríguez-Genó, C. F. Sistema automático de predicción a mesoescala de cuatro ciclos diarios. 2014, Technical Report, Instituto de Meteorología de Cuba, <https://doi.org/10.13140/RG.2.1.2888.1127>.

- 191 2. Sierra-Lorenzo, M., Borrajero-Montejo, I., Ferrer-Hernández, A. L., Hernández-Valdés, R., Morfa-Ávalos, Y., Morejón-Loyola,
192 Y., Hinojosa-Fernández, M. Estudios de sensibilidad del sispi a cambios de la pbl, la cantidad de niveles verticales y, las
193 parametrizaciones de microfísica y cúmulos, a muy alta resolución. 2017, Technical Report, Instituto de Meteorología de
194 Cuba, <http://dx.doi.org/10.13140/RG.2.2.29136.00005>.
- 195 3. Alfonso Aguila, S.; Fuentes Barrios, A.; Sierra Lorenzo, M. Evaluation of the Nowcasting and very Short-Range Prediction
196 System of the National Meteorological Service of Cuba. Environ. Sci. Proc. 2021, 8, 36. <https://doi.org/10.3390/ecas2021-10353>.
- 197 4. Skamarock, W. C., Klemp, J. B., Dudhia, J., Gill, D. O., Liu, Z., Berner, J., Wang, W., Powers, J. G., Duda, M. G., Barker, D. M.,
198 and Huang, X.-Y. A Description of the Advanced Research WRF Version 4.1. 2019. NCAR Tech. Note NCAR/TN-556+STR, 145
199 pp. <https://doi.org/10.5065/1dfh-6p97>.
- 200 5. Hernández, R. Asimilación de observaciones meteorológicas con el modelo físico – matemático ARPS. 2013. Trabajo Diploma.
201 Instituto Superior de Tecnologías y Ciencias Aplicadas. La Habana, Cuba.
- 202 6. Ferrer, A.L. Simulación numérica de tornados en Cuba. 2013. Trabajo Diploma. Instituto Superior de Tecnologíaas y Ciencias
203 Aplicadas. La Habana, Cuba Armas, E. Asimilación de Observaciones de Satélites Meteorológicos en el modelo WRF. 2015.
204 Trabajo Diploma. Instituto Superior de Tecnologías y Ciencias Aplicadas. La Habana, Cuba.
- 205 7. Ferrer, A.L. and Borrajero, I. (2019): “Estudio Preliminar Para La Implementación De La Asimilación De Datos De Radares Y
206 Satélites Meteorológicos En Pronósticos Numéricos A Muy Alta Resolución Sobre La Región Occidental De Cuba
207 <http://repositorio.geotech.cu/jspui/bitstream/1234/4186/1/Estudio%20preliminar%20para%20la%20implementaci%C3%B3n%20de%20la%20asimilaci%C3%B3n%20de%20datos%20de%20radares.pdf>. Informe de resultado científico presentado en el
208 Consejo Científico del Instituto de Meteorología de Cuba.
209
- 210 8. Fernández, D. Corrección de errores sistemáticos en la inicialización del modelo WRF utilizando asimilación de datos de
211 radar. 2019. Trabajo Diploma. Instituto Superior de Tecnologías y Ciencias Aplicadas. La Habana, Cuba.
- 212 9. González, P.M., Ferrer, A.L., Aguiar, D.C. and Sierra, M. Determinación del sistema de asimilación de datos a utilizar, así
213 como de las observaciones meteorológicas que se emplearán en SisPI. 2021. Informe de resultado científico presentado en el
214 Consejo Científico del Instituto de Meteorología de Cuba.
- 215 10. Aguiar, D. Comparación entre los métodos de asimilación de datos de radar del WRFDA para su implementación en SisPI.
216 2021. Trabajo Diploma. Instituto Superior de Tecnologías y Ciencias Aplicadas. La Habana, Cuba
- 217 11. Min, K. and Kim, Y. Assimilation of null-echo from radar data for QPF. 2016. 17th Annual WRF Users' Workshop. Posters
218 Session: Development and Testing for WRF Data Assimilation. P78.
- 219 12. Lee, J.-W.; Min, K.-H.; Lee, Y.-H.; Lee, G. X-Net-Based Radar Data Assimilation Study over the Seoul Metropolitan Area.
220 Remote Sens. 2020, 12, 893. <https://doi.org/10.3390/rs12050893>
- 221 13. Barker, D. M., Huang, W., Guo, Y-R., Bourgeois, A. J., and Xiao, Q. N. A Three-Dimensional (3DVAR) Data Assimilation
222 System For Use With MM5: Implementation and Initial Results. 2004. Mon. Wea. Rev., 132, 897–914.
223 <http://n2t.net/ark:/85065/d79g5ndw>
- 224 14. Lee, YH., Min, KH. High-resolution modeling study of an isolated convective storm over Seoul Metropolitan area. Meteorol
225 Atmos Phys 131, 1549–1564 (2019). <https://doi.org/10.1007/s00703-019-0657-2>